A novel adaptive extended kalman filtering and electrochemical-circuit combined modeling method for the online ternary battery state-of-charge estimation

Jiang, Cong; Wang, Shunli; Wu, Bin; Etse-Dabu, Bobobee; Xiong, Xin

Published in:
International Journal of Electrochemical Science

DOI (link to publication from Publisher):
10.20964/2020.10.09

Publication date:
2020

Document Version
Publisher's PDF, also known as Version of record

Int. J. Electrochem. Sci., 15 **(2020)** 9720 – 9733, doi: 10.20964/2020.10.09

International Journal of ELECTROCHEMICAL SCIENCE
www.electrochemsci.org

A Novel Adaptive Extended Kalman Filtering and Electrochemical-Circuit Combined Modeling Method for the Online Ternary Battery state-of-charge Estimation

Cong Jiang[1], *Shunli Wang*[1,2,*], *Bin Wu*[1], *Bobobee Etse-Dabu*[1], *Xin Xiong*[1]

[1] School of Information Engineering, Southwest University of Science and Technology, Mianyang, 621010, China
[2] Department of Energy Technology, Aalborg University, Pontoppidanstraede 111 9220 Aalborg East, Denmark
[*]E-mail: 497420789@qq.com

Received: 6 May 2020 / *Accepted:* 30 July 2020 / *Published:* 31 August 2020

Lithium-ion batteries are used more and more extensively, and the state-of-charge estimation of lithium-ion batteries is essential for their efficient and reliable operation. In order to improve the accuracy and reliability of battery state-of-charge estimation, the Thevenin model was established and the parameters of the least square method model with forgetting factor were used for online identification estimation. To reduce the impact of noise, an adaptive extended Kalman algorithm is developed by combining Sage-Husa adaptive filter with extend Kalman filter algorithm for SOC estimation. The experimental results compared with ampere-time integral method and standard extend Kalman filter method, the improved adaptive extend Kalman filter algorithm has good convergence speed, higher estimation accuracy and stability. The initial SOC error is 5%, and the root mean square error of extend Kalman filter SOC estimation algorithm is 0.0124. In contrast, the root mean square error of the proposed adaptive extend Kalman filter SOC estimation algorithm is 0.0109.

Keywords: lithium-ion battery; state-of-charge; adaptive extend Kalman filter; recursive least squares with forgetting factor; online parameters identification;

1. INTRODUCTION

Due to the high energy density and long cycle life of lithium-ion battery, it currently plays an important role in electric vehicles (EV) and energy storage [1-3]. However, when the lithium-ion battery is overcharged or over discharged, it may even cause fire and explosion [4]. In order to ensure the safe and reliable operation of lithium batteries, a battery management system (BMS) is essential. One of the main and core functions is SOC estimation. SOC can quantify the remaining battery power of the current

battery and remind personnel how long the battery can work before charging. Specifically, SOC is defined as the percentage of remaining capacity relative to its maximum available capacity, and its function is similar to the fuel gauge of gasoline-powered vehicles on EV [5, 6]. The SOC of lithium-ion battery is affected by factors such as temperature, charge and discharge status, self-discharge, and aging. Internal chemical reactions are variable and their characteristics are highly non-linear. These characteristics make SOC estimation difficult. Because the battery itself has strong nonlinear characteristics and complex application conditions, accurate SOC estimation is still an urgent problem to be solved.

At present, many researchers have studied the SOC estimation of lithium-ion battery and lots of methods have been proposed to estimate the SOC. The existing SOC estimation methods are mainly divided into the following categories: (1) direct measurement method; (2) model-based estimation method; (3)data-driven estimation method [7, 8].

(1) Direct measurement method: The direct measurement method mainly includes coulomb counting method and open circuit voltage (OCV) method. Knowing the initial value of SOC, the SOC value can be obtained by integrating the current. This method is called coulomb counting method or ampere-hour integral method which is an open-loop method. It is sensitive to the initial value and interference, and will cause the cumulative error to be uncorrectable. The relationship between open circuit voltage and SOC can be obtained by a fixed discharge rate, and then the value of the corresponding SOC is found in the relationship curve using the known OCV [9]. This method is called the open circuit voltage method [10]. Although the method can measure the value of SOC [11], the battery must be allowed to stand for more than one hour to start measurement, and the battery itself is susceptible to temperature and reproductive quality [12, 13]. In the same OCV, the SOC differs under varied conditions. Therefore, it is not suitable for SOC estimation in operation.

(2) Data-driven estimation method: Data-driven control methods use the input-output data of the system to develop an estimator. Since these methods do not require an accurate plant model, the estimations and assumptions introduced in the plant modeling step are omitted [7]. The typical algorithms include the fuzzy controller, the neural network [14-17], and the support vector machine [18]. But data driven estimation method suffers from problems like extensive training, difficult online adaption, and high computational effort [19].

(3) Model-based estimation method: With the development of battery research, many battery models for the power LIB have been proposed [20-24]. The most commonly used models can be roughly summarized into three types: electrochemical models (EM), equivalent circuit models (ECM) and electrochemical impedance models (EIM). In the model-based estimation method, the battery model is generally expressed as state equations. Several state observers have been applied to the models separately, including extended Kalman filter (EKF), unscented Kalman filter (UKF) sliding mode observer (SMO), particle filter (PF), H-infinity observer and their improved algorithms [2, 8, 16, 25-32].

Accurate model is essential for SOC estimation of lithium-ion battery. The battery model parameters are affected by the environment and aging. In order to avoid the problem of adaptability of offline parameter identification, the on-line parameter identification of battery in Thevenin model where ohmic internal resistance, polarization resistance, polarization capacitance and other parameters are based on the recursive least squares with forgetting factor (FFRLS). The Thevenin equivalent circuit

model that adapts to changes is accurately established. Both the Kalman algorithm and the EKF algorithm treat system noise as white noise, ignoring the noise characteristics in practical applications, resulting in the noise affecting the accuracy of SOC estimation. The noise is adjusted by Sage-Husa adaptive filter, and the adaptive extended Kalman filter (AEKF) is a combined algorithm.

The rest of this paper is organized as follows. The mathematical theoretical analysis is conducted in section 2 including a definition of SOC, modeling of the LIB and AEKF algorithm. In section 3, the experiments are illustrated as well as its estimation effect results. The conclusions and future works are finally reported in Section 4.

Table 1. List of symbols used in the paper

Symbol	Full-name	Symbol	Full-name
BMS	Battery management system	EV	Electric vehicle
SOC	State of charge	ECM	Equivalent circuit model
FFRLS	recursive least squares with forgetting factor	RC	Resistor-capacitor
PF	Particle filter	UKF	Unscented Kalman filter
KF	Kalman filter	AEKF	Adaptive extended Kalman filter
EKF	Extended Kalman filter	ANN	Artificial neural network
HPPC	Hybrid Pulse Power Characteristic	CC-CV	Constant current-constant voltage
OCV	Open circuit voltage	RMSE	Root mean square error

2. MATHEMATICAL ANALYSIS

The basic definition of SOC is introduced firstly in this section. Then, the established Thevenin equivalent model and the corresponding parameter identification method are described. Finally, the proposed AEKF is introduced in detail and the framework of SOC estimation is given.

2.1. Definition of state-of-charge

The SOC of lithium-ion battery characterizes the remaining capacity, and it is defined as the ratio of the remaining capacity to the maximum available capacity which can be expressed as Eq. (1) [8].

$$\begin{cases} S_t = \dfrac{C_t}{C_{MAX}} \times 100\% \\ S_t = S_0 - \dfrac{\int_{t_0}^{t} \eta I(t) \eta dt}{C_{MAX}} \end{cases} \tag{1}$$

In the Eq. (1), S_t is the current estimated SOC. C_t is the remaining battery capacity. C_{MAX} is the maximum available capacity when the battery is fully charged. S_0 is the initial SOC when the estimation process starts, h denotes the Coulombic efficiency, and $I(t)$ is the load current (assumed discharging is positive).

2.2. Battery Equivalent Model Construction

In order to accurately estimate the SOC, a reliable battery model is needed. The general lithium battery equivalent models mainly include neural network models, electrochemical models and the equivalent circuit models [33]. Since the equivalent circuit model (ECM) has the advantages of clear physical meaning and simple calculation, many researchers use it for SOC estimation [20-25]. Compared the effects of different order models on the estimation results, and the results show that ECMs with Thevenin and second-order RC models are consistently more accurate and reliable than other models [34]. Therefore, considering model complexity, Thevenin equivalent circuit model is selected for equivalent modeling in many research [1, 4, 8, 19, 23]. The specific circuit is shown in Fig.1 [21].

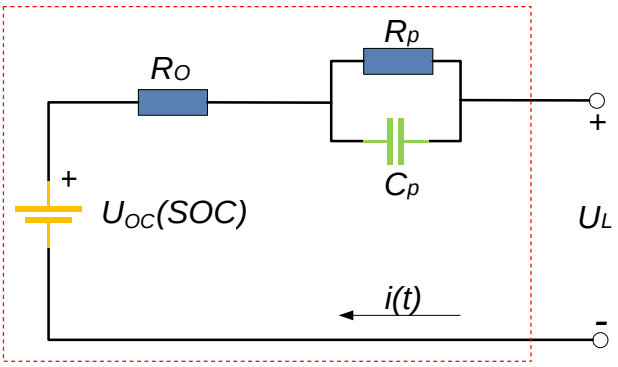

Figure 1. Thevenin equivalent circuit model

In Fig.1, U_{oc} represents the open-circuit voltage of the lithium-ion battery, R_O represents the ohmic internal resistance, R_O characterizes the ohmic effect of the battery, R_P represents the polarization resistance of the lithium battery, C_P represents the polarization capacitance, and the RC network characterizes the polarization phenomenon of the lithium-ion battery, *i(t)* indicates the load current, where the discharge direction is positive, and U_L indicates the closed-circuit voltage when the battery is externally connected. The circuit equation shown in Fig.1 can be listed according to the circuit law as shown in Eq. (2) [35].

$$\begin{cases} U_L = U_{OC} - I(t)R_o - U_p \\ \dfrac{dU_p}{dt} = \dfrac{I}{C_p} - \dfrac{U_p}{R_p C_p} \end{cases} \tag{2}$$

Combined with the state-of-charge definition, the state-space variable $x_k = \left[S_k, U_{p,k}\right]^T$, the input variable $u_k = I_k$, and the output variable $y_k = U_{L,k}$ are selected. The discrete state-space equation can be obtained as shown in Eq. (3) [36].

$$\begin{cases} X_k = \begin{bmatrix} S_k \\ U_{p,k} \end{bmatrix} = \begin{bmatrix} 1 & 0 \\ 0 & e^{-\Delta t/\tau} \end{bmatrix} \begin{bmatrix} S_k \\ U_{p,k} \end{bmatrix} + \begin{bmatrix} -\eta \dfrac{\Delta t}{C_{\max}} \\ R_p(1-e^{-\Delta t/\tau}) \end{bmatrix} I_k + w \\ U_{L,k} = U_{OC}(S_k) - U_{p,k} - I_k R_o + v \end{cases} \quad (3)$$

Wherein, Δt is the sampling interval time and it has little influence on the SOC estimation results during the simulation process, but the smaller the test the actual computing power of the BMS equipment. $\tau = R_p C_p$, w is the state error and v is the measurement error, which are the zero-mean white noises of the covariance matrices Q and R, respectively. where the subscript k represents the value of the corresponding variable at time step k.

2.3. The battery OCV model

Improvement in the accuracy and robustness of OCV model can also significantly increase the accuracy of SOC estimation. The OCV can be characterized by the state variable SOC relationship, which the nonlinear function can be obtained from. The simplified electrochemical model (SE), whose terms is shown in Eq. (4) [8].

$$U_{OC,k} = K_0 - K_1 S_k - K_2 / S_k + K_3 \ln S_k + K_4 \ln(1 - S_k) \quad (4)$$

2.4. Model parameters online identification

With the battery's working environment, working conditions, aging, etc., battery model parameters will change, offline parameter identification is difficult to accurately reflect changes in battery characteristics. In order to better follow the battery model parameter changes, the recursive least squares with forgetting factor is used to perform online parameter identification of the battery model [19]. According to the circuit knowledge, the Eq. (5) can be obtained.

$$G(s) = \frac{U_L(s) - U_{OC}(s)}{I(s)} = R_o + \frac{R_p}{1 + R_p C_p s} \quad (5)$$

The open circuit voltage U_{OC} is the voltage at which the battery is stable at both positive and negative terminals when the battery is left for a long time. Experiments have shown that the voltage after the battery has been allowed to stand for 40 minutes is stable and can be considered to be equal to the open circuit voltage of the battery. Using the bilinear transform rule, the discrete-time form of the system transfer function in Eq. (6) can be obtained as:

$$G(z) = \frac{U_d(z)}{I(z)} = \frac{a_2 + a_3 z^{-1}}{1 + a_1 z^{-1}} \quad (6)$$

Where

$$\begin{cases} a_1 = \dfrac{T - 2R_pC_p}{T + 2R_pC_p} \\ a_2 = \dfrac{R_oT + R_pT + 2R_oR_pC_p}{T + 2R_pC_p} \\ a_3 = \dfrac{R_oT + R_pT - 2R_oR_pC_p}{T + 2R_pC_p} \end{cases} \tag{7}$$

Define

$$\begin{cases} \varphi_k = \left[-U_d(k-1) \quad I(k) \quad I(k-1)\right] \\ \theta_k = \left[a_1 \quad a_2 \quad a_3\right] \end{cases} \tag{8}$$

The vector θ(k) in Equation (8) can be further solved using the recursive least square algorithm with forgetting factor λ (typically λ = [0.95, 1]) formulated as:

$$\begin{cases} L_k = \dfrac{P_{k-1}\varphi_k^T}{\lambda + \varphi_k P_{k-1}\varphi_k^T} \\ P_k = \lambda^{-1}(P_{k-1} - L_k\varphi_k P_{k-1}) \\ \theta_k = \theta_{k\text{-}1} + L_k(U_d(k) - \varphi_k\theta_{k\text{-}1}) \end{cases} \tag{9}$$

The value of the parameters involving R_o, R_p and C_p can be obtained by calculation such as Eq. (10).

$$\begin{cases} R_o = \dfrac{a_2 - a_3}{1 - a_1} \\ \tau = R_pC_p = \dfrac{(1-a_1)T}{2 + 2a_1} \\ R_p = (1 + \dfrac{2\tau}{T})a_2 - \dfrac{2R_o\tau}{T} - R_o \\ C_p = \dfrac{\tau}{R_p} \end{cases} \tag{10}$$

2.5. Adaptive Extend Kalman filter

The current SOC estimation method is mainly based on the equivalent model, combined with the Kalman filter (KF) algorithm and its extended algorithm [2, 8, 16, 25-32], as well as fuzzy logic and neural network related algorithms [14-17]. KF algorithm is one of the most widely used intelligent algorithms, and is usually used in practical situations, such as path planning, target tracking, and SOC estimation of lithium batteries. The basic principle of the algorithm is to take the minimum mean square error as the best estimation criterion, by establishing a state equation and an observation equation model, a state space model of signals and noise is used to introduce the relationship between the state variables

and the observed variables. Time estimates and observations of the current time update the estimates of the state variables [20].

The Kalman filter algorithm estimates the properties of the SOC of the lithium battery by calculating the SOC using the amperage time integration method, and uses the measured voltage value to correct the SOC value obtained by the amperage time integration method. When the SOC of a battery is estimated by Kalman filtering, a suitable equivalent battery model needs to be established, and the accuracy of the Kalman algorithm depends on the accuracy of the battery model. When the Kalman filtering method is used to estimate the SOC of a battery, the battery is considered to be a power system, the SOC is the state of the system, the charge and discharge current of the battery is used as the input to the system, and the terminal voltage is used as the output. The state of the system is continuously updated by the error of the observed value of the terminal voltage and the estimated value of the SOC, thereby obtaining the SOC value of the minimum variance estimate.

The model is the premise basis for the application of the algorithm. Because the model parameters are affected by battery aging, environment, working conditions, etc. The above-mentioned FFRLS method is used in this paper to perform online real-time identification and update of battery model parameters. The mathematical expression of the state space equation of the Thevenin equivalent circuit model of the lithium battery in Eq. (3) can be simplified as shown in Eq. (11).

$$\begin{cases} x_k = f(x_{k-1}, u_{k-1}) + w_k \\ y_k = h(x_k, u_k) + v_k \end{cases} \tag{11}$$

The functions of f (*) and h (*) are nonlinear equations. The upper equation in Eq. (11) is the state equation, where x_k is the n-dimensional system state vector at time point k, and v is the ndimensional system noise vector. The function $f(x_k, u_k)$ is a non-linear state transition function. The second equation in equation (11) is an observation equation, where y is an observation vector, and v is a multi-dimensional system interference vector at time point k. The function $h(x_k, u_k)$ is a non-linear measurement function. The above function can be explored by using the Tailor method on the prior estimation point x_k of the state x_{k+1} [31]. The higher-order components of the process can be ignored, and linear approximations of off (*) and h (*) can be used as shown below:

$$\begin{cases} f(x_k, u_k) \approx f(x_{k|k-1}, u_k) + \left.\dfrac{\partial f(x_k, u_k)}{\partial x_k}\right|_{x_k = x_{k|k-1}} (x_k - x_{k|k-1}) \\ h(x_k, u_k) \approx h(x_{k|k-1}, u_k) + \left.\dfrac{\partial h(x_k, u_k)}{\partial x_k}\right|_{x_k = x_{k|k-1}} (x_k - x_{k|k-1}) \end{cases} \tag{12}$$

The estimation process of the Kalman filter algorithm includes time update and measurement update. The time update process is also known as the forecast process. It is a one-step prediction of the current state variable and provides a prior estimation process for the next moment. The measurement update process is the process of feeding back observations and correcting deviations. The EKF algorithm formula is as follows.

1) The initial condition of the filter equation is:

$$x_0 = E(x), P_0 = \mathrm{Var}(x) \tag{13}$$

2) State vector estimation time update:

$$x_{k|k-1} = f(x_{k-1}, u_{k-1}) \tag{14}$$

3) State covariance update time update:

$$P_{k|k-1} = FP_{k-1}F^T + Q_k \tag{15}$$

4) Calculate Kalman gain coefficient:

$$K_k = P_{k|k-1}H^T(HP_{k|k-1}H^T + R_k) \tag{16}$$

5) State vector measurement update:

$$x_k = x_{k|k-1} + K_k(y_k - h(x_{k|k-1}, u_k)) \tag{17}$$

6) update state covariance matrix:

$$P_k = (I - K_k H)P_{k|k-1} \tag{18}$$

In the above formula, $x_{k|k-1}$ is direct time estimate at time k, x_{k-1} is the optimal estimate state value at the last moment. P_k is the covariance update of x_k, Q_k is the covariance of process noise w, K_k is the Kalman gain coefficient. R_k is the covariance of observation noise v. Sage-Husa adaptively updates the noise variables, and by comparing the final estimated value with the estimated value. The calculation process of the estimator-related quantities is shown in Eq. (19).

$$\begin{cases} \tilde{y}_k = y_k - h(x_k, u_k) - R_{k-1} \\ Q_k = \dfrac{1}{k}\sum_{i=0}^{k-1}\left(K_k\tilde{y}_k\tilde{y}_k^T K_k^T + P_k - FP_{k|k-1}F^T\right) \\ R_k = \dfrac{1}{k}\sum_{i=0}^{k-1}\left(\tilde{y}_k\tilde{y}_k^T - HP_{k/k-1}H^T\right) \end{cases} \tag{19}$$

In order to make the estimation of noise more accurate and to avoid the influence on the observed value, this paper considers the noise at the previous moment and the moment at the same time, and adopts the weighting coefficients d_k and $d_k = (1-b)/(1-b^{k+1})$, n = 0,1, ... k. b is the forgetting factor. In practice, the smaller the value of b, the smaller the impact at the previous moment; if the value of b is small, the estimated noise will oscillate, so it can be determined according to the specific situation. Then the calculation formula of the noise matrix is as shown in Eq. (20).

$$\begin{cases} Q_k = (1-d_{k-1})Q_{k-1} + d_{k-1}\left(K_k\tilde{y}_k\tilde{y}_k^T K_k^T + P_k - FP_{k/k-1}F^T\right) \\ R_k = (1-d_{k-1})R_{k-1} + d_{k-1}\left(\tilde{y}_k\tilde{y}_k^T - HP_{k/k-1}H^T\right) \end{cases} \tag{20}$$

The process noise and observation noise are corrected by Eq. (14), and the AEKF algorithm is combined with Eq. (13) to Eq. (20).

In this paper, the battery is modeled equivalently, and the estimated results of EKF and the AEKF algorithm are compared based on the established model. The complete iterative calculation flowchart is shown in Fig.2.

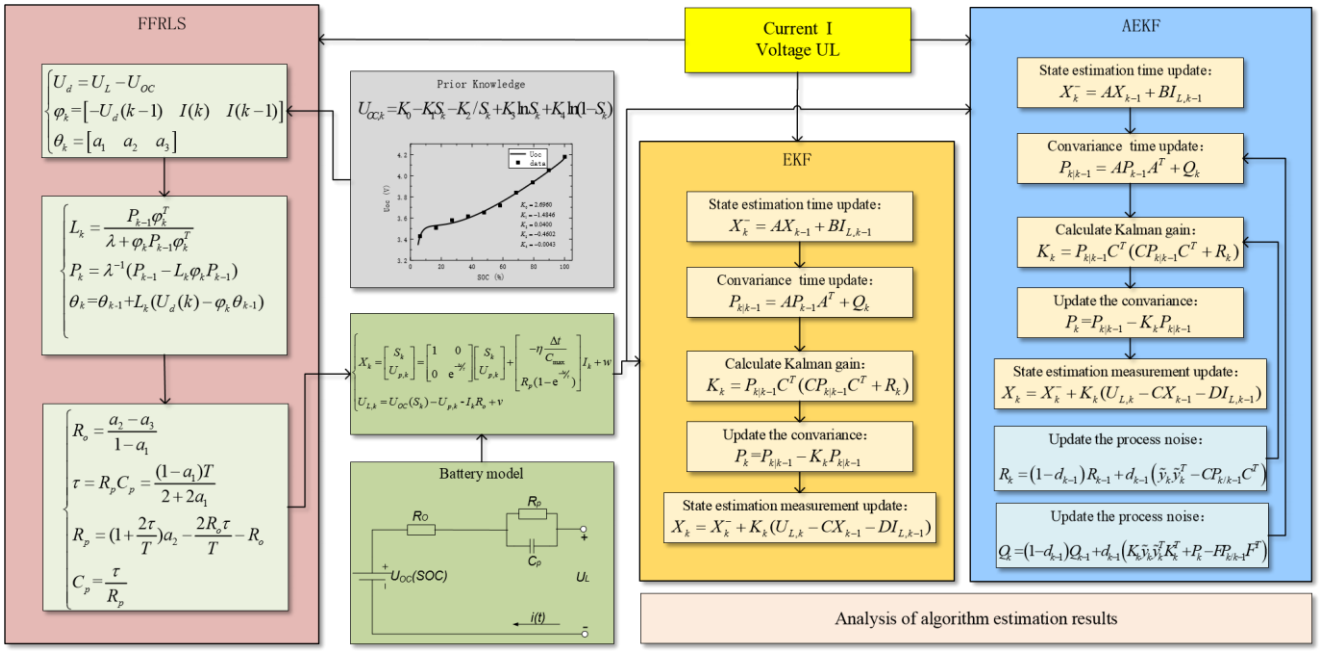

Figure 2. The iterative SOC estimation flowchart

3. EXPERIMENTAL ANALYSIS

3.1. Test platform construction

Table 2. Basic technical parameters of the battery

Cell nominal capacity/Ah	50	Standard charge current	1C
Rated voltage/V	3.65	Standard discharge current	3C
Charge cut-off voltage/V	4.2±0.05	Maximum load current	5C
Discharge cutoff voltage/V	2.65±0.05	Internal resistance/ mΩ	0.8
Size: l * w * h/ mm	148×27×93	Working temperature/℃	-20~60

All the data in this article are derived from the comparison and verification for ternary lithium battery LFP50Ah for parameter identification at 25 degrees Celsius. The basic information of the battery is shown in Table 2. The battery test equipment used is CT-4016-5V100A-NTFA, and the temperature box is BTT-331C of Bell Test Equipment Co., Ltd.

The LFP50Ah ternary power lithium battery was used as the experimental object, and its rated capacity was 50 ampere (Ah), the charge cut-off voltage was 4.2V, and the discharge cut-off voltage

was 2.75V. The test equipment is the sub-source CT-4016-5V100A-NTFA, which has a maximum current of 100A, and a maximum voltage of 5V. The thermostat model is BTT-331C.

3.2. Battery test and results analysis

The above-mentioned lithium battery as an experimental object was placed in a 25 ° C incubator, connected to a test device, and a capacity measurement experiment. An HPPC experiment was performed on the battery according to the following steps [37]. The experimental current voltage curve is shown in Fig. 3.

(1) Charge the battery with constant current and constant voltage. The process is to charge the battery with a constant current of 1C (here 50A) to a cut-off voltage of 4.2V, and change to a constant voltage of 4.2V until the charging current is less than 0.05C (here 2.5A) is considered complete. Let the battery have a rest for 1 hour.

(2) Constant-current discharge of the battery to a cut-off voltage of 2.7V and a discharge current of 1C (here 50A) . Let the battery have a rest for 1 hour.

(3) Repeat steps (1) and (2) three times, and take the average value of the three discharges as the maximum available capacity of the battery. The measured discharge capacity here is 48.07Ah, 48.26Ah, 48.15Ah, and the average is 48.16Ah.

(4) After performing step (1) on the lithium battery, SOC = 1.

(5) Discharge the experimental battery at a constant current of 1C for 10s, leave it for 40s, and charge at 1C for 10s, then leave it.

(6) Discharge the battery with a current value of 50A for 6 minutes to decrease the battery SOC to the next SOC point and leave it for 30 minutes.

(7) Repeat steps (5) (6) 9 times to obtain the complete current-voltage curve as shown in the Fig. 3(b) below.

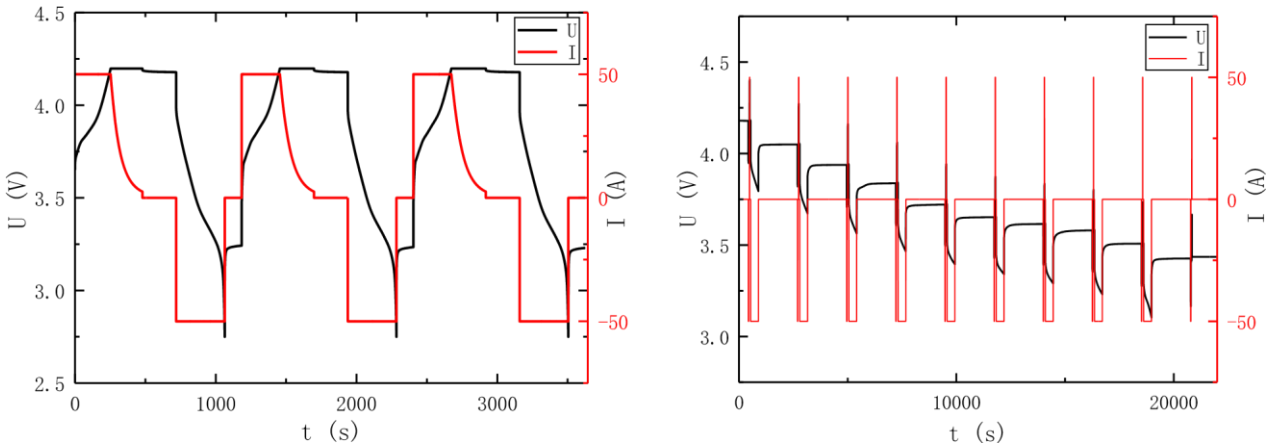

(a) Battery discharge capacity test (b) Hybrid Pulse Power Characteristic

Figure 3. Battery current voltage curve

Fig. 4(a) shows the U_{OC}-*SOC* relationship. After the lithium-ion battery has a rest for 30 minutes, the internal reaction ceases. We can think that the terminal voltage is equal to the open circuit voltage at this time. So 10 open-circuit voltage data points can be obtained from Fig. 3(b). According to Eq. (4), the data is fitted by least square method to obtain the function curve Uoc1(Here, when SOC=1 is regarded as 0.9999). The fitting parameter results are shown in Table 3.

Table 3. Basic technical parameters of the battery

parameter	K_0	K_1	K_1	K_1	K_1
value	2.6960	-1.4846	0.0400	-0.4602	-0.0043

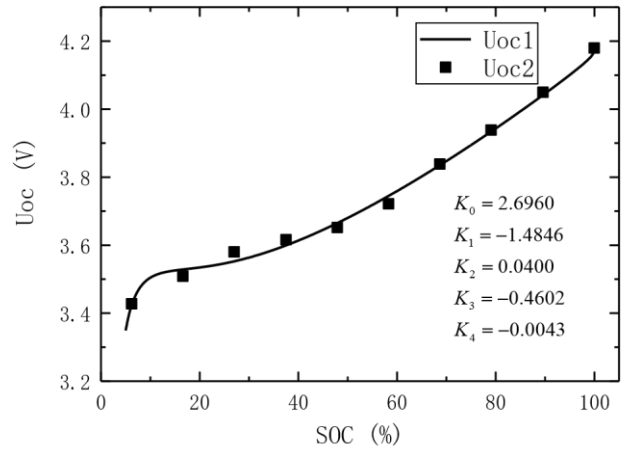

(a) The Uoc and SOC relationship diagram

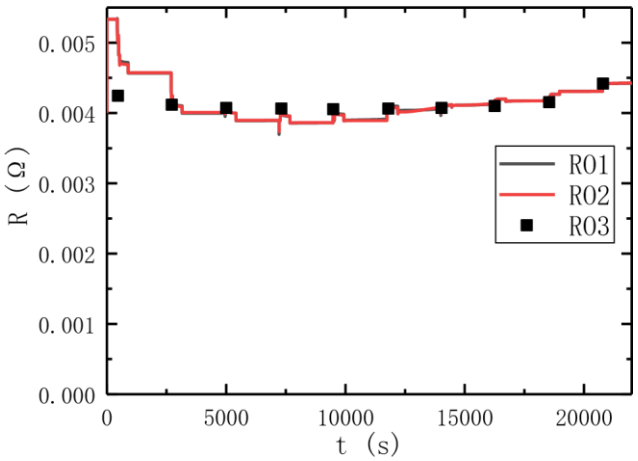

(b) ohmic resistance RO identification result

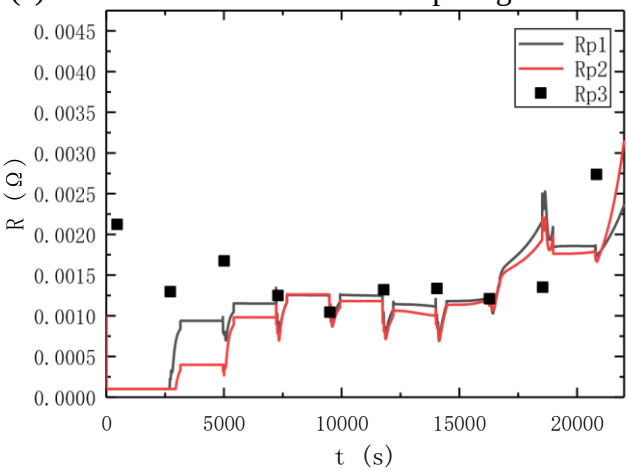

(c) Polarization resistance R_P identification result

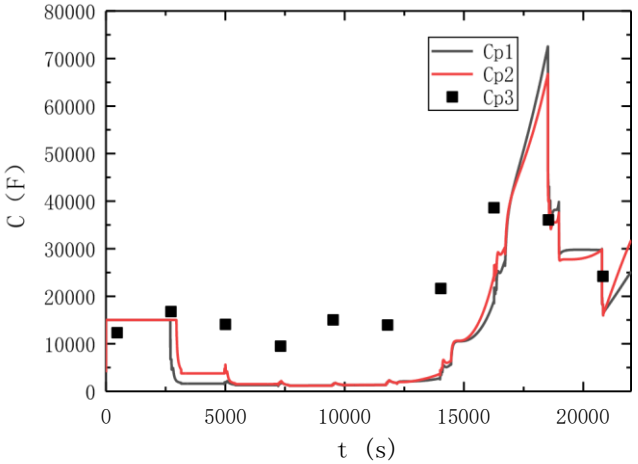

(d) Polarization capacitance C_P identification result

Figure 4. Model parameters identification results

In Fig.3, *U* represents the terminal voltage of the lithium ion battery, *I* represents the charging and discharging current. Use the current and voltage in Fig. 3 as input data and program it in Matlab according to section 2 mathematical analysis. The battery Thevenin model parameters change as shown in Fig. 4.

R_O R_P C_P In Fig. 4 (b), Fig. 4 (b) and Fig. 4 (b), R_{O1}, R_{P1} and C_{P1} are parameters change curves online identified by FFRLS algorithm for identification combined with EKF for SOC estimation. R_{O2}, R_{P2} and C_{P2} are parameters change curves online identified by FFRLS algorithm for identification combined with EKF for SOC estimation. R_{O3}, R_{P3} and C_{P3} are parameter data for offline identification. It can be seen from the figure that due to the 5% error in the initial SOC setting of the EKF and AEKF algorithms, there is a certain deviation in the parameter values. As the algorithm iterates, the model parameter values begin to approach offline data.

3.3. Analysis of state-of-charge estimation results

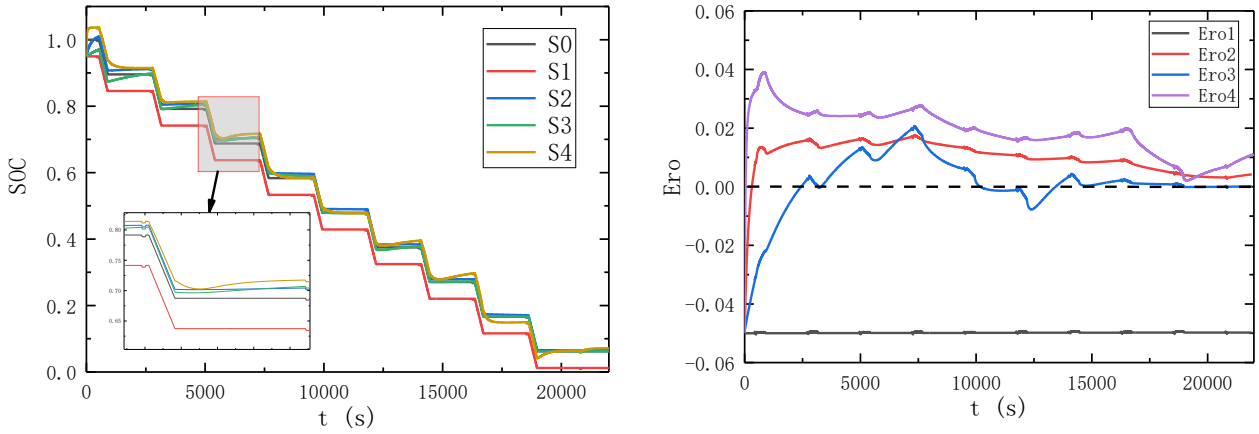

(a) SOC estimation results curve (b) SOC estimation error curve

Figure 5. Comparison of SOC estimation results

Based on the HPPC operating conditions in Fig. 4(b), the initial SOC error of lithium ion battery is set at 5%, and the SOC estimation is performed using the ampere-hour integration method, EKF and AEKF respectively. The SOC estimation results are shown in Fig. 5.

In Fig. 5 (a), S0 is the reference lithium-ion battery SOC. S1 is the estimation results based on ampere-hour integration method, S2 and S3 is the estimation results by EKF and AEKF respectively based on online Thevenin model. S4 is the estimation results by EKF based on offline Thevenin model. Fig. 5(b) is the SOC estimation error curve obtained by subtracting the reference SOC curve S0 from S1, S2, S3 and S4 respectively. The ampere-hour integration method cannot correct the initial SOC deviation, and the error remains at about 5%. EKF and AEKF algorithms can correct the initial error, and the error gradually converges with the iteration. The RSME of extend Kalman filter SOC estimation algorithm online parameter identification is 0.0124. In contrast, the RMSE of the proposed adaptive extend Kalman filter SOC estimation algorithm is 0.0109 and AEKF algorithm has higher accuracy. Furthermore, the RMSE of EKF SOC estimation algorithm based on offline parameter identification is 0.0183. The accuracy of SOC estimation based on online parameter identification is higher.

4. CONCLUSIONS

In this study, Thevenin model was established and the parameters of the least square method model with forgetting factor were used for online identification estimation. In order to improve the accuracy and reliability of battery state-of-charge estimation, Thevenin model was established and the parameters of the least square method model with forgetting factor were used for online identification estimation. In order to reduce the impact of noise, an adaptive extended Kalman algorithm is obtained by combining Sage-Husa adaptive filter with extended Kalman filter algorithm for SOC estimation. The results show that FFRLS can effectively identify the battery Thevenin model parameters online and better than offline parameter identification. Compared with ampere-time integral method and standard extend Kalman filter method, the improved adaptive extended Kalman filter algorithm has good convergence speed, higher estimation accuracy and stability under the condition of HPPC.

ACKNOWLEDEGMENTS
The research was supported by National Natural Science Foundation of China (No. 61801407).

References

1. Y. Wang, X. Zhang, C. Liu, R. Pan and Z. Chen, *J Power Sources*, 389 (2018) 93.
2. Z. H. Chen, H. Sun, G. Z. Dong, J. W. Wei and J. Wu, *J Power Sources*, 414 (2019) 158.
3. S. Akagi, S. Yoshizawa, M. Ito, Y. Fujimoto, T. Miyazaki, Y. Hayashi, K. Tawa, T. Hisada and T. Yano, *Int J Elec Power*, 116 (2020).
4. W. J. Zhang, L. Y. Wang, L. F. Wang and C. L. Liao, *J Power Sources*, 402 (2018) 422.
5. Y. J. Zheng, M. G. Ouyang, X. B. Han, L. G. Lu and J. Q. Li, *J Power Sources*, 377 (2018) 161.
6. C. Bian, H. He, S. Yang and T. Huang, *J Power Sources*, 449 (2020).
7. R. Xiong, J. Cao, Q. Yu, H. He and F. Sun, *IEEE Access*, 6 (2018) 1832.
8. H. Pan, Z. Lü, W. Lin, J. Li and L. Chen, *Energy*, 138 (2017) 764.
9. Y. Ma, Y. Chen, X. Zhou and H. Chen, *Ieee Trans.Control Syst.Technol.*, 27 (2019) 1788.
10. A. B. Ahmad, C. A. Ooi, D. Ishak and J. Teh, *Ieee Access*, 7 (2019) 131.
11. K. D. Hoang and H. H. Lee, *Ieee T Ind Electron*, 66 (2019) 1883.
12. D. T. Liu, L. Li, Y. C. Song, L. F. Wu and Y. Peng, *Int J Elec Power*, 110 (2019) 48.
13. L. Zheng, J. Zhu, G. Wang, D. D.-C. Lu and T. He, *Energy*, 158 (2018) 1028.
14. X. Dang, L. Yan, K. Xu, X. Wu, H. Jiang and H. Sun, *Electrochimica Acta*, 188 (2016) 356.
15. M. S. H. Lipu, M. A. Hannan, A. Hussain and M. H. M. Saad, *J Renew. Sustain. Ener.*, 9 (2017).
16. Y. Tian, R. Lai, X. Li, L. Xiang and J. Tian, *Applied Energy*, 265 (2020).
17. M. Jiao, D. Wang and J. Qiu, *J Power Sources*, 459 (2020).
18. Y. Z. Wang, Y. L. Ni, N. Li, S. Lu, S. D. Zhang, Z. B. Feng and J. G. Wang, *Energy Sci Eng*, 7 (2019) 2797.
19. Z. Zeng, J. Tian, D. Li and Y. Tian, *Energies*, 11 (2018) 59.
20. S. L. Wang, J. Y. Shi, C. Fernandez, C. Y. Zou, D. K. Bai and J. C. Li, *Energy Sci Eng*, 7 (2019) 546.
21. B. Xia, X. Zhao, R. de Callafon, H. Garnier, T. Nguyen and C. Mi, *Applied Energy*, 179 (2016) 426.
22. J. Q. Linghu, L. Y. Kang, M. Liu, B. H. Hu and Z. F. Wang, *Energies*, 12 (2019).
23. Z. Wei, J. Zhao, D. Ji and K. J. Tseng, *Applied Energy*, 204 (2017) 1264.

24. H. Mu, R. Xiong, H. Zheng, Y. Chang and Z. Chen, *Applied Energy*, 207 (2017) 384.
25. F. Yan, C. Zhang, C. Du and C.-H. Cheng, *Int. J. Electrochem. Sci.*, 13 (2018) 12360.
26. J. Hou, Y. Yang, H. He and T. Gao, *Appl Sci-Basel*, 9 (2019).
27. B. Yuan Chaochun, B. Wang, H. Zhang, C. Long and H. Li, *Int. J. Electrochem. Sci.*, 13 (2018) 1131.
28. M. Ye, H. Guo and B. Cao, *Applied Energy*, 190 (2017) 740.
29. Q. Zhu, M. G. Xu, W. Q. Liu and M. Q. Zheng, *Energy*, 187 (2019) 11.
30. X. Lai, L. He, S. Wang, L. Zhou, Y. Zhang, T. Sun and Y. Zheng, *J Clean Prod*, 255 (2020).
31. S. Wang, C. Fernandez, L. Shang, Z. Li and H. Yuan, *Trans. Inst. Meas. Control*, 40 (2018) 1892.
32. H. Li, X. Wang, A. Saini, Y. Zhu and Y.-P. Wang, *Int. J. Electrochem. Sci.*, 15 (2020) 3807.
33. E. Chemali, P. J. Kollmeyer, M. Preindl and A. Emadi, *J Power Sources*, 400 (2018) 242.
34. Y. Wang, Z. Chen and C. Zhang, *Applied Energy*, 194 (2017) 688.
35. X. Xin, S.-L. Wang, C.-M. Yu, J. Cong and J. Coffie-Ken, *Int J Electrochem Sci.*, 15 (2020) 2226.
36. X. Lai, Y. Zheng and T. Sun, *Electrochimica Acta*, 259 (2018) 566.
37. Y. Wang, C. Liu, R. Pan and Z. Chen, *Energy*, 121 (2017) 739.